Low-Frequency Modes of Peptides and Globular Proteins in Solution Observed by Ultrafast OHD-RIKES Spectroscopy

Gerard Giraud, Jan Karolin, and Klaas Wynne
Department of Physics, University of Strathclyde, Glasgow G4 0NG, Scotland, United Kingdom

ABSTRACT The low-frequency (1–200 cm^{-1}) vibrational spectra of peptides and proteins in solution have been investigated with ultrafast optical heterodyne-detected Raman-induced Kerr-effect spectroscopy (OHD-RIKES). Spectra have been obtained for di-L-alanine (ALA(2)) and the α-helical peptide poly-L-alanine (PLA) in dichloroacetic acid solution. The poly-L-alanine spectrum shows extra amplitude compared to the di-L-alanine spectrum, which can be explained by the secondary structure of the former. The globular proteins lysozyme, α-lactalbumin, pepsin, and β-lactoglobulin in aqueous solution have been studied to determine the possible influence of secondary or tertiary structure on the low-frequency spectra. The spectra of the globular proteins have been analyzed in terms of three nondiffusive Brownian oscillators. The lowest frequency oscillator corresponds to the so-called Boson peak observed in inelastic neutron scattering (INS). The remaining two oscillators are not observed in inelastic neutron scattering, do therefore not involve significant motion of hydrogen atoms, and may be associated with delocalized backbone torsions.

INTRODUCTION

Conformational changes in proteins by definition involve the vibrational normal modes of the macromolecule. There are thousands of modes in a typical protein, ranging from high-frequency well-defined localized modes to very low frequency delocalized modes. In many if not most cases, protein functionality involves conformational changes of the molecular structure. It is useful to make a distinction between two classes of motions (Hammes-Schiffer, 2002): Promoting motions take place on the timescale of biochemical reactions (e.g., milliseconds), are diffusive, and influence the activation free-energy barrier by changing the tertiary structure. Dynamical motions determine the probability of barrier crossing in the transition state, take place on a femtosecond to picosecond timescale, and involve changes in the secondary structure and individual residues. Here we are concerned with the dynamical motions, which can be observed spectroscopically.

Recent theoretical work has shown that picosecond fluctuations in the secondary structure are crucial in determining reaction rates in proteins. For example, it has been calculated (Fischer et al., 2001) that ligand binding to an enzyme causes softening of low-frequency delocalized modes. Similarly, instantaneous normal-mode calculations on enzymes (Levitt et al., 1985) show the presence of collective modes with large amplitude around the active site. Structural fluctuations around the active site on a picosecond timescale have been shown (Zhou et al., 1998) to be a mechanism for an enzyme to achieve substrate specificity. The picosecond flickering between the α- and PPII-helix conformation of hydrated helices is thought (Barron et al., 1997) to be important for enzyme activity and protein folding. However, experimental verification of these results is lacking.

It is not necessarily useful to think of conformational changes in terms of vibrational normal modes. For example, if these modes were to exchange energy with the heat bath quickly or were highly anharmonic, the normal-mode picture would be ineffective. Experimental evidence indicates that a normal-mode picture is useful in understanding dynamical motions. For example, it has been shown (Xie et al., 2002) that the lifetime of vibrational excitations of collective modes at 115 cm^{-1} in bacteriorhodopsin exceeds 500 ps. Numerous ligand-dissociation experiments (Groot et al., 2002; Rosca et al., 2002) in heme proteins have shown coherent excitation of low-frequency vibrational modes (40–160 cm^{-1}), indicating a strong coupling with the reaction. Photon-echo studies (Jimenez et al., 2002) have shown that charge rearrangement on an antigen is coupled to a number of low-frequency modes in the antibody it is bound to. Studies of photoactive yellow protein (Xie et al., 2001) have found evidence for ''protein quakes,'' that is, processes involving conformational changes triggered and driven by a local structural ''fault.''

Thus, low frequency (1–200 cm^{-1}) collective vibrational modes form part of the reaction coordinates of the functional motions of active proteins. The obvious next step is determining the nature of these collective modes experimentally. X-ray crystallography and NMR can measure static structure or at most temperature factors but provide no information about modes, and therefore dynamics and function. Recent ultrafast time-resolved two-dimensional IR techniques have been applied to the amide I region of small peptides and proteins (Jung et al., 2000; Woutersen and Hamm, 2001; Zanni and Hochstrasser, 2001; Zanni et al., 2001) allowing the observation of the coupling between the different amide oscillators in the molecule. The dynamical vibrational motions involved in protein activity take place on

Submitted April 22, 2003, and accepted for publication June 10, 2003.

Address reprint requests to Klaas Wynne, 107 Rottenrow, Glasgow G4 0NG, Scotland, UK. Tel.: 44-141-548-3381; E-mail: klaas.wynne@phys.strath.ac.uk.

0006-3495/03/09/1903/11 $2.00

a (sub)picosecond timescale and therefore correspond to the microwave to far-infrared range. Infrared spectroscopy, especially in the 1–200 cm^{-1} or terahertz range (Beard et al., 2002), suffers from strong water absorption that makes meaningful study of hydrated biomolecules very difficult.

Intramolecular vibrations have been investigated at an early stage with Raman spectroscopy on dry films of proteins (Genzel et al., 1976). The technique used here is optical heterodyne-detected Raman-induced Kerr-effect spectroscopy or OHD-RIKES (Smith and Meech, 2002). This technique has proven to be superior to IR and Raman spectroscopy at low frequencies (<400 cm^{-1}) and its high signal-to-noise ratio allows a detailed analysis of the spectra. In recent work (Giraud and Wynne, 2002), we have shown for the first time that OHD-RIKES can be used to study low-frequency modes in proteins and peptides.

Here we will describe the application of OHD-RIKES to the study of the low-frequency vibrational spectra of a number of model systems. In the first half, the influence of the secondary structure on the low frequency modes will be discussed by comparing the spectra of the dimer di-L-alanine (ALA(2)) with the α-helical peptide poly-L-alanine (PLA). In the second half, the spectra of four globular proteins will be discussed, two predominantly α-helical: lysozyme and α-lactalbumin, and two mainly β-sheet: pepsin and β-lactoglobulin. Comparison of the OHD-RIKES spectra with previous Raman and inelastic neutron-scattering (INS) spectra and theoretical work, will allow a partial assignment of the low-frequency spectra.

EXPERIMENTAL SETUP

Optical heterodyne-detected Raman-induced Kerr-effect spectroscopy experiments have been reported previously (Smith and Meech, 2002) and the details of our experimental setup have been described in detail elsewhere (Giraud et al., 2003). Therefore, only the basic principles of the experiment will be summarized here. OHD-RIKES is a polarization-spectroscopy technique that provides a signal linear in the third-order optical response of the sample. Information is obtained regarding ultrafast solvent/protein dynamics by measuring the time response of a transient birefringence that is induced in the sample by a polarized femtosecond optical pulse. Our setup uses very short (20-fs) stable laser pulses and the signal is obtained with a shot-noise limited balanced-detection system. The ultrafast OHD-RIKES measurements have been carried out using linearly polarized optical pulses centered at 800 nm. The laser beam was split into a pump beam ($\sim$80%) and a probe beam ($\sim$20%) by a beam splitter, and the pump beam was optically delayed using a 50-nm resolution stepper motor. Polarizers were placed in both arms to obtain a 45° angle between pump and probe-beam polarizations. A 6-cm focal-length lens has been used to focus the two beams into the sample. Phase-sensitive detection has been achieved with a chopper and lock-in amplifier. The pulse width has been measured at the sample position as 20 fs FWHM ($sech^2()$) by two-photon absorption in a GaP PIN photodiode.

Balanced detection presents some advantages compared to the traditional technique (McMorrow et al., 1988). In our setup, the probe beam is circularly polarized with a quarter-wave plate after the sample. Parallel and perpendicular components are separated with a Glan-Thompson polarizer and sent to a pair of photodiodes wired up for balanced detection (Wynne et al., 2000). Because the signal is obtained by electronically subtracting the horizontal from the vertical component of the probe beam, it is possible to reduce the effect of random fluctuations of the laser power and achieve a significant improvement in the signal-to-noise ratio. It can be shown using a Jones-matrix analysis (Giraud et al., 2003) that by balancing with either a quarter- or a half-wave plate, a signal either purely due to birefringence or purely due to dichroism is measured.

Because of the signal produced by the solvent, the study of proteins or peptides in solution using OHD-RIKES requires a large amount of biological material, typically 0.2 g for 0.5 ml solvent. The peptides di-L-alanine and poly-L-alanine have been studied in dichloroacetic acid (DCA) and four globular proteins have been studied in water. The solubility properties of peptides chains decreases with the number of amino acids. Although the dimer ALA(2) is soluble in water, PLA has low solubility in aqueous and organic solvents but does dissolve well in organic acids such as dichloroacetic acid and trifluoroacetic acid (TFA) (Gold and Miller, 1999). Up to 0.1 g dry protein could be dissolved in 0.5 ml TFA. The bulky CHCl2 group of the DCA molecules prevents the breaking and unfolding of the α-helical peptide (Bamford et al., 1956; Ferretti and Paolillo, 1969). Therefore, the configuration of PLA in DCA is α-helical with 3.6 residues per turn as confirmed by Raman optical-activity measurements (L. D. Barron and I. McColl, personal communication, 2002). PLA (molecular weight 1000–5000, $\approx$30 residues) was obtained from ICN Biomedicals (Aurora, OH) and ALA(2) from Sigma-Aldrich (Poole, UK). Both have been used without further purification. The globular proteins lysozyme, pepsin, β-lactoglobulin and α-lactalbumin have been obtained from Sigma-Aldrich and were studied close to their saturation concentration of 0.25 g dry protein in 0.5 ml double distilled water. Filtering of the samples with syringe filters (0.22-μm pore diameter, Millipore, Watford, UK) was found to be essential to prevent light scattering.

DATA ANALYSIS

Analysis of the OHD-RIKES data can be performed either in the time or in the frequency domain. Relaxation processes are more easily visualized in the time domain but for analyzing the molecular dynamics, it is easier and more meaningful to work in the frequency domain. The first part of this section details how the data have been sampled and

transformed to the frequency domain, and the second part concentrates on the analysis of the spectrum.

The OHD-RIKES signal is measured in the time domain and therefore any analysis has to start there. Because ultrashort pulses are not instantaneous, the observed signal $S(t)$ in the ultrafast OHD-RIKES experiment is the convolution of the second-order autocorrelation function of the laser pulse $G_2(t)$ with the molecular nonlinear impulse response $R(t)$ (McMorrow et al., 1988):

$$S(t) \propto \int_{-\infty}^{t} d\tau\, R(t-\tau) G_2(\tau). \quad (1)$$

The impulse-response function is obtained by Fourier deconvolution of the experimental signal yielding $R(\omega)$ (McMorrow and Lotshaw, 1990). Because the nuclear (vibrational) response in the time domain cannot be instantaneous whereas the electronic response (in the Born-Oppenheimer approximation) is, the imaginary part of $R(\omega)$ is purely related to the nuclear part of the transient birefringence (McMorrow, 1991). The resulting spectrum is equal to the low-frequency depolarized Raman spectrum multiplied by a Bose thermal-occupation factor (Cho et al., 1993):

$$\mathrm{Im}\, R(\omega) = R_{\mathrm{DRS}}(\omega)[1 - \exp(-\hbar\omega/k_{\mathrm{B}}T)]. \quad (2)$$

In the experiments described here, data were recorded from -1 ps to 5 ps. Examples of the signals in the time domain are given in Fig. 1. A sharp peak corresponding to the electronic response of the sample arises at time zero, followed by the librational ultrafast dynamics in the first picosecond, and a subsequent slow exponential tail attributed to diffusional processes. Before transformation to the frequency domain, careful manipulation of the raw time-domain data is required to maximize the signal-to-noise ratio as well as the physical accuracy of the spectrum. Because the spectrum is obtained by Fourier transformation of the OHD-RIKES time-domain signal, any noise present in the long-time tail of the signal (due to a decrease of the signal strength at long delays) is observed in the low frequency part of the spectrum. This can be avoided by applying a window function to the data (Press et al., 1992). Here the OHD-RIKES signal was multiplied with a Gaussian function $w(t) = \exp(-(t-t_0)^2/2\sigma^2)$, where t_0 is the zero time delay, $\sigma = \tau/2\sqrt{2}$ and $\tau = 4ps$. This procedure results in an effective spectral resolution of 9 cm^{-1} FWHM. A valid spectrum is only obtained if the time reference (zero delay between pump and probe pulses) of the autocorrelation and OHD-RIKES signals are identical. Because the autocorrelation and birefringence signals have to be measured separately, their respective zero delay position is slightly shifted, if only by a few femtoseconds typically. It is therefore necessary to match the reference time of the two signals. This has been done empirically by correcting the zero delay of the signal (± 5 fs) to obtain a spectrum that is positive from 0 cm^{-1} to the highest possible frequency while minimizing any background. However, this is still the greatest potential source of systematic errors and becomes progressively worse at higher frequencies (larger than a few hundred wavenumbers).

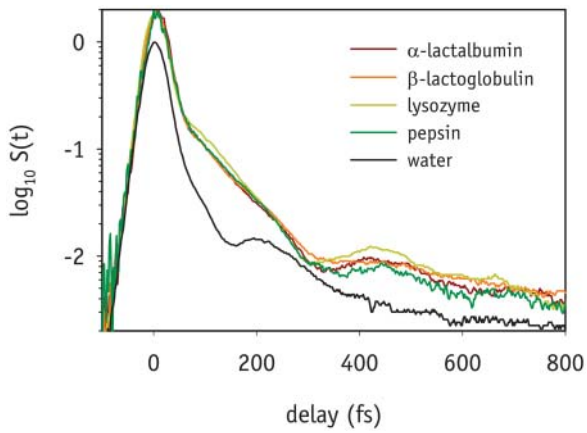

FIGURE 1 OHD-RIKES experimental time-domain data of the four globular proteins studied and pure water. The amplitude of the pure-water data has been scaled proportionally to the known water content of the samples.

Once the spectrum has been obtained by deconvolution, two points must be taken into account before analysis: the normalization of the spectra and the solvent contribution to the signal. The amplitude of an experimental OHD-RIKES spectrum is somewhat arbitrary, mostly because of small power fluctuations of the laser and minor misalignments of the setup due to temperature fluctuations. To compare the relative amplitudes of the different spectra, it is necessary to normalize the signal. In the time domain, the signal at zero delay is purely electronic. It has been found that the electronic response in pure DCA is the same as in solutions of peptides in DCA. As a normalization procedure, the electronic responses were forced to be equal. Similarly, it has been found that the electronic response of water is on average 80% of that in solutions of proteins in water. Again, this has been used for normalization.

In principle, the low-frequency vibrational spectra of the peptides and proteins can be obtained by simply subtracting the pure solvent spectrum in proportion. However, the solutes may be expected to interact with the surrounding solvent thereby locally changing the solvent properties. Recent studies have shown that hydration water is confined by a protein substrate and behaves differently from bulk water (Crupi et al., 2002; Paciaroni et al., 1999). An inelastic neutron-scattering (INS) experiment on crystallized lysozyme (Bon et al., 2002) has revealed that the water molecules close to a protein can be divided into two populations. The first mainly corresponds to the first hydration shell, in which water molecules diffusively reorient themselves 5- to 10-fold slower than in bulk solvent, and diffuse by jumping between hydration sites with a long-range self-diffusion coefficient reduced by about a factor of five compared to bulk solvent. The second group corresponds to water molecules further

away from the surface of the protein in a second incomplete hydration layer with a long-range translational diffusion coefficient reduced by about a factor of 50. Therefore, OHD-RIKES spectra that result from the subtraction of their bulk solvent component include motion of the protein as well as motion of the solvent molecules interacting with the surface of the protein. The solvent subtraction has been done in proportion to the relative amount of peptide/protein by weight in the sample. The solute-solvent ratio for the peptide and protein samples was 20:80 and 33:66 respectively. Thus, the ALA(2) and PLA spectra have been obtained by subtracting 80% of the pure DCA spectrum and the protein spectra by subtracting 66% of the pure water spectrum. For convenience, the resulting spectra will be referred to as ''solvent free'' (SF) in the text.

A protein such as lysozyme consists of about a hundred residues corresponding to a thousand-odd atoms each with three translational degrees of freedom. Although in principle this should result in $3N - 6$ or thousands of normal modes, in practice the ultrafast (50 fs to 5 ps) response can be modeled by a small number of low-frequency harmonic modes much like is seen in liquids (Cho et al., 1993; G. Giraud and K. Wynne, unpublished results). The reason for this is fast and weakly coupled fluctuations that damp the modes and cause the vibrational lines to be homogeneously broadened and overlapping. The result is that the spectrum appears to consist of a relatively small number of homogeneously broadened modes that determine the ultrafast dynamics. Three parameters describe each mode: the frequency of the mode, its damping rate, and its amplitude.

The data from the OHD-RIKES experiments have been analyzed in terms of the Brownian-oscillator model. This model has been described in detail in the literature (Cho et al., 1993) and only the strategic points will be discussed here. The nuclear motion is modeled by harmonic oscillators where each satisfies a generalized Langevin equation whose response function in the frequency domain is given by

$$C(\omega) = (4/M)([\gamma - 2i\omega]^2 + 4\Omega^2)^{-1}, \qquad (3)$$

with $\Omega \equiv (\omega_0^2 - \gamma^2/4)^{1/2}$ where γ denotes the damping rate, M the reduced mass, and ω_0 the undamped frequency of the mode under consideration. The experimental low-frequency spectra ($\leq$200 cm^{-1}) of the globular proteins have been fitted with up to five Brownian-oscillator functions as given by Eq. 3. As the experimental spectra have been fitted to such a large number of functions using such a large number of parameters, a proper analysis of the uncertainties in the parameters is essential. All data have been fitted using a nonlinear least-squares fitting program based on the simplex algorithm (Press et al., 1992). The resulting fit parameters and associated uncertainties are presented in Table 1.

The indicated uncertainties in the parameters are only due to lack of fit and do not include any systematic errors. The uncertainties in the fit parameters are 68.3% joint-confidence intervals (Seber and Wild, 1989) and therefore take into account uncertainties resulting from correlations between the parameters.

TABLE 1 Amplitude, frequency, and damping parameters of the Brownian oscillators listed with their respective uncertainties for the four proteins studied

Amplitude	ω (cm^{-1})	γ (cm^{-1})
	Pepsin	
18 ± 5	28 ± 3	87 ± 17
132 ± 30	65 ± 6	idem
258 ± 60	100 ± 4	idem
	α-Lactalbumin	
24 ± 6	33 ± 3	95 ± 12
72 ± 15	62 ± 5	idem
291 ± 63	98 ± 2	idem
	β-Lactoglobulin	
0.18 ± 0.12	7 ± 2	7 ± 5
24 ± 8	48 ± 5	75 ± 7
135 ± 26	83 ± 5	idem
111 ± 32	110 ± 5	idem
	Lysozyme	
0.2 ± 0.1	6 ± 1	5 ± 3
32 ± 4	45 ± 2	58 ± 5
162 ± 16	82 ± 2	idem
154 ± 13	112 ± 2	idem

RESULTS

Here we will present the OHD-RIKES spectra of a number of peptides and proteins in solution. The spectra of the dimer ALA(2) and the peptide PLA in DCA have been studied to determine the effect of secondary structure on the low-frequency vibrational spectra. In comparison to our previous study (Giraud and Wynne, 2002), the present data have been refined and our analysis entirely reviewed. In addition, the spectra of four globular proteins in aqueous solution have been studied to determine whether different types of secondary structure (e.g., α-helical, random coil, etc.) give rise to different spectra and whether any spectral features corresponding to tertiary structure can be observed.

Polypeptides

Fig. 2 presents the spectra of ALA(2) and PLA in a solution with DCA after subtraction of the bulk solvent spectrum (solvent-free, SF). Fig. 2 *c* compares the spectra of SF PLA and SF ALA(2) and shows the (double) difference spectrum.

It is observed for both the SF ALA(2) and SF PLA spectra that their low-frequency vibrational band covers a large range of frequencies with amplitude at frequencies as high as 200 cm^{-1} compared to an upper limit of $\sim$100 cm^{-1} for most organic solvents. This suggests a relatively strong interaction between solvent and solute molecules as has been observed, for example, in highly polar ionic liquids (Giraud

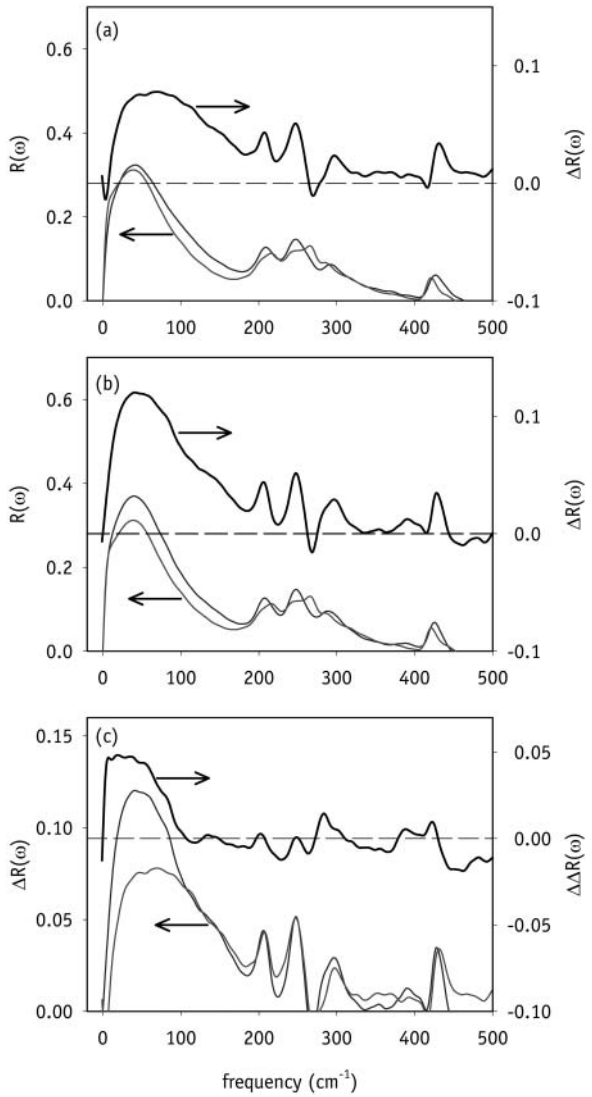

FIGURE 2 OHD-RIKES spectra of ALA(2) and PLA in a solution with DCA. (*a*) The spectra of bulk DCA (*top*) and a solution of ALA(2) in DCA (*middle*) and the difference spectrum (*bottom*) obtained by subtracting the appropriate fraction of the bulk solvent spectrum from the spectrum of the solution. (*b*) Idem, for PLA. (*c*) The difference spectra for ALA(2) (*top*) and PLA (*middle*) from panels *a* and *b* and the double difference spectrum (*bottom*).

et al., 2003). What could be the reason for such strong interactions in these solutions? The dominant species of alanine in aqueous solution is the zwitterionic form. Zwitterion formation in aqueous solution occurs by means of the ionization of the carboxylic-acid and amino groups and the same process, although perhaps more slowly, is likely to occur in DCA. The zwitterionic solutes are expected to interact strongly with each other and with the aqueous environment. In addition, hydrogen bonding can occur between the solutes and the solvent in both aqueous solution and solution with DCA. Together, the strong coulombic and hydrogen-bond interactions are the main reason for the broad low-frequency band observed in SF ALA(2) and SF PLA. This hypothesis is supported by the similar OHD-RIKES spectra of ALA(2) in aqueous and DCA solution (See Fig. 3). The oscillatory features seen in Fig. 2 between 200 and 300 cm^{-1} are the result of intramolecular Raman bands in DCA shifting to lower frequency on addition of peptide. These band shifts are likely due to the perturbation of hydrogen bonds through the carboxylic groups in DCA affecting the low frequency intramolecular modes involving the heavy chlorine atoms (Nakabayashi et al., 1999).

The low-frequency band of SF PLA displays a peak at 60 and a shoulder at 140 cm^{-1}. Polarized Raman and infrared spectra of oriented films of α-helical PLA (Lee and Krimm, 1998a) reveal a number of bands around 100 cm^{-1} that have been assigned to delocalized backbone torsions in some cases mixed with hydrogen-bond stretching (Lee and Krimm, 1998b). In comparison, the low-frequency band of SF ALA(2) presents a single featureless band. Fig. 2 *c* shows that the spectra of SF ALA(2) and SF PLA match above 100 cm^{-1} and that extra amplitude appears in the case of PLA below 100 cm^{-1}. As both samples contain an equal concentration of solute by weight, this strongly suggests (but does not prove) that the SF PLA spectrum is the combination of a signal proportional to its primary structure (alanine) that would be identical to the ALA(2) spectrum, with a signal proportional to its secondary structure (α-helix). In this interpretation, the (double) difference spectrum in Fig. 2 *c* represents the component of the SF PLA spectrum that originates in the secondary structure.

Observations using the Raman optical-activity technique have suggested (Barron et al., 1997) that residues in disordered loop regions of molten globule-like states flicker between close lying regions of the Ramachandran surface at a rate of $\sim 10^{12}$ Hz. This is approximately the rate for hydrogen-bond rearrangements in bulk water but interestingly it is also approximately the peak of the double difference spectrum in Fig. 2 *c*.

The amplitude of the OHD-RIKES spectrum scales with the square of the derivative of the polarizability tensor (Cho

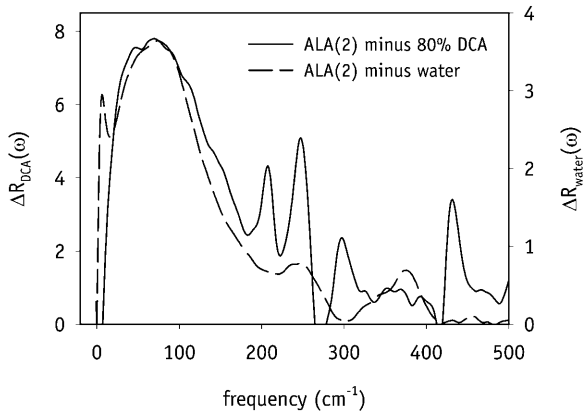

FIGURE 3 OHD-RIKES spectra of ALA(2)-obtained after subtraction of the bulk solvent spectrum in aqueous and DCA solution.

et al., 1993). Therefore, the extra amplitude below 100 cm^{-1} observed in SF PLA must be due to either an additional mode or modes that change the polarizability along their vibrational coordinates or due to an overall increase in the polarizability in the helical conformation. As discussed above, ALA(2) in solution most likely occurs in the zwitterionic form resulting in a large concentration of bare charges. In the case of PLA, only the ends of the chain can be ionized, decreasing the concentration of bare charges compared to ALA(2). A further difference is that α-helical PLA has a large number of intramolecular hydrogen bonds at the expense of intermolecular hydrogen bonds with the solvent molecules. However, it is difficult to see how these differences in the concentration of bare charges or the number of intramolecular hydrogen bonds could explain the extra amplitude below 100 cm^{-1}.

In ALA(2) in solution, the permanent dipole-moment vectors of the peptide bond are randomly oriented in space. On the other hand, PLA forms a regular α-helical structure allowing vectorial addition of the peptide permanent dipole-moment vectors resulting in a large total permanent dipole moment and a considerable local electric field (Daune, 1999; Hol et al., 1978). No data are available concerning the effect such a strong field might have on the polarizability of individual amino-acid residues. However, considering the delocalization of the π-bond in the amide link in amino acids, we surmise that a strong electric field can modify the electronic properties of amino-acid residues and induce a greater anisotropy in the polarizability of individual residues. An increased anisotropy in the polarizability implies increased amplitude in the OHD-RIKES (and Raman) spectrum for librational modes. Furthermore, the polarizability will depend on the local electric field, which in turn depends on the secondary structure. Therefore, any vibrational mode that changes the secondary structure will also be Raman active. This picture is consistent with the assignment of low-frequency modes in PLA to delocalized backbone torsions mixed with hydrogen-bond stretching (Lee and Krimm, 1998b). It is also consistent with the picture that solvent molecules can form transient hydrogen bonds with the helix causing a flickering between close lying secondary structures (Barron et al., 1997). In summary, it appears that the formation of secondary structure implies the emergence of extra amplitude in the vibrational spectrum below 100 cm^{-1}. The remaining questions are whether it is possible to distinguish different types of secondary structure from the low-frequency OHD-RIKES spectra and whether tertiary structure results in additional features.

Globular proteins

The OHD-RIKES spectra of four globular proteins in aqueous solution have been investigated. The four proteins have been chosen based on their predominant secondary structure: lysozyme and α-lactalbumin are mostly α-helical and β-lactoglobulin and pepsin are mostly β-pleated. However, each of these four proteins has a mixture of secondary-structure types as can be found by analyzing data from the protein data bank (Berman et al., 2000). The ratio α-helical/β-pleated/random coil is for lysozyme 43:5:52 (Vaney et al., 1996), for α-lactalbumin 33:17:50 (McKenzie and White, 1991), for pepsin 13:59:28 (Sielecki et al., 1990), and for β-lactoglobulin 6:45:49 (Kuwata et al., 1999).

Fig. 4 shows the raw OHD-RIKES spectra of the four globular proteins in aqueous solution from 0 to 800 cm^{-1} together with the spectrum of pure water scaled according to the experimentally determined water content (one-third protein and two-thirds water by mass). At the highest frequencies (about >600 cm^{-1}), the spectra start to curve upwards or downwards due small residual zero time-delay errors or minor pulse-width fluctuations. It can be seen that the spectra of α-lactalbumin and pepsin approach the spectrum of water around a frequency of 400 cm^{-1}, validating the procedure of subtraction of the bulk solvent spectrum to obtain the SF spectrum. However, the spectra of lysozyme and β-lactoglobulin only approach the water spectrum at ~700 cm^{-1}. Simple subtraction of the bulk water spectrum not only leaves a plateau in the spectra of lysozyme and β-lactoglobulin between 300 and 600 cm^{-1}, but also a clear shoulder at 170 cm^{-1} that is at exactly the same frequency as one of the peaks of the water spectrum. This has led us to believe that the lysozyme and β-lactoglobulin samples contain more water than initially thought, possibly because of the different solubility properties and the different amounts of protein-bound water. Lysozyme and α-lactalbumin have an almost identical structure (McKenzie and White, 1991), however, their different solvent exposed side chains give them altered solubility properties. It is known that proteins can have between 0.2 and 0.7 g strongly associated (bound) water per g protein (Pethig, 1992). At large concentrations of protein, a small difference in bound

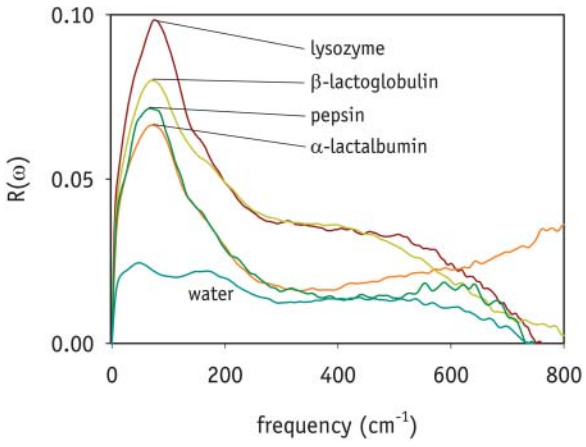

FIGURE 4 Raw OHD-RIKES spectra of the four globular proteins lysozyme, α-lactalbumin, β-lactoglobulin, and pepsin in aqueous solution, along with the spectrum of water scaled in proportion to the sample water content.

water concentration can have a significant effect on the raw spectrum. Consequently, the water content of the samples was reevaluated and subtracted individually for the four protein samples. This has been done empirically by scaling the water spectrum to minimize the background of the SF spectrum. The resulting spectra are shown in Fig. 5. The validity of the data above $\sim$300 cm^{-1} should be regarded with a certain degree of suspicion. However, the broad band above 200 cm^{-1} in β-lactoglobulin and lysozyme has recently been seen in another experiment as well (Eaves et al., 2003). Spontaneous Raman spectroscopy could in principle be used to obtain more reliable spectra in this region.

All four SF protein spectra in Fig. 5 show a similar broad band with maximum amplitude at around 80 cm^{-1}. Lysozyme and β-lactoglobulin on the one hand and pepsin and α-lactalbumin on the other show a common appearance. This shows that there is no clear and direct relation between the proportion of the various types of secondary structure in a protein and its low-frequency OHD-RIKES spectrum. In other words, a protein with large α-helical content can give rise to an OHD-RIKES/Raman spectrum that appears similar to that of a protein with large β-pleated sheet content. The broad band peaking around 300 cm^{-1} in the samples of lysozyme and β-lactoglobulin in Fig. 5 is difficult to explain. In all likelihood, this band is simply the result of an artifact of the bulk-solvent spectrum subtraction procedure combined with zero time-delay errors. Finally, the main difference between the two sets of spectra is the appearance of larger amplitude around 30 cm^{-1} in pepsin and α-lactalbumin. This difference, which cannot be explained as an artifact of the experiment, is again not related to the proportion of secondary structure and must therefore depend on other properties of the protein.

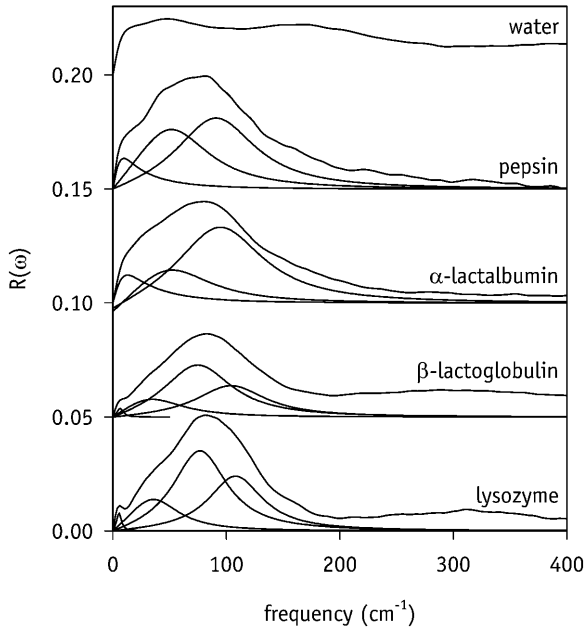

FIGURE 5 OHD-RIKES spectra of the four globular proteins studied after subtraction of the hand-scaled water spectrum. The curves have been shifted vertically for clarity. The spectra have been fitted with the Brownian-oscillator model as described in the text.

Fig. 5 shows the four SF spectra of the proteins between 0 and 200 cm^{-1} accompanied by fits to a multiple Brownian-oscillator model. Fitting these spectra is nontrivial and fraught with pitfalls because the spectra are relatively unstructured, have a fair amount of random noise, and contain systematic errors because of zero time-delay errors, subtraction artifacts, and small ripples originating as artifacts from the Fourier-transform procedure. Therefore, one is forced to put constraints on the parameters to get meaningful results. Each Brownian oscillator (See Eq. 3) has three parameters: an amplitude, a frequency, and a damping rate. The damping is a result of the coupling between the Brownian oscillator and the bath. In Kubo relaxation theory (Kubo, 1969; Wood and Strauss, 1990), the damping rate is described by two parameters: the characteristic timescale of fluctuations of the bath τ and the strength of the coupling to the bath Δ. In the fast-modulation or homogeneous-broadening limit, the relaxation rate is given by $\gamma = \Delta^2\tau$. In the case under consideration here, the bath is the protein itself and therefore it is reasonable to assume that the timescale of bath fluctuations is the same for all Brownian oscillators. In addition, it is quite reasonable to assume that the coupling to the bath will be the same for similar types of motions. Therefore, if the broad band observed in the spectra between 0 and 150 cm^{-1} is caused by similar librations and vibrations of the peptide backbone, one should be able to fit these to a number of Brownian oscillators with identical damping rates. Clearly, this is a contentious assumption but it is the only way the data can be fitted to theory with some degree of accuracy.

Table 1 shows the parameters of the fits shown in Fig. 5. The spectra of pepsin and α-lactalbumin could be fitted with three Brownian oscillators. In the case of pepsin, a damping rate for the three oscillators of 87 $\pm$ 17 cm^{-1} was found, in the case of α-lactalbumin, a damping rate of 95 $\pm$ 12 cm^{-1} was found. The fit to the spectra of β-lactoglobulin and lysozyme required four Brownian oscillators. Keeping the damping rate of all four oscillators the same resulted in an unsatisfactory fit. It appears that the lowest frequency component in these two spectra is of a different origin, perhaps diffusion of solvent exposed side chains. Therefore, the lowest frequency component was fitted to a Brownian oscillator with an independent damping rate. The damping rate for the remaining three Brownian oscillators was found to be 75 $\pm$ 7 cm^{-1} for β-lactoglobulin and 58 $\pm$ 5 cm^{-1} for lysozyme. Therefore, except for the diffusive component in two spectra, all four spectra exhibit the same behavior and can be fitted to three Brownian oscillators with similar damping rates of $\sim$80 cm^{-1}. This consistency provides some confidence in the validity of these fits. The biggest question remains for now, however: Whether the three oscillators found in each case have any physical meaning and, if so, to what type of motion in the protein they can be assigned to.

DISCUSSION

As indicated earlier, the solvent-free OHD-RIKES spectra presented here represent vibrational motion of both the protein/peptide itself as well as motion of solvent molecules close to and perturbed by the solute. Hydration water around a protein exhibits dynamical properties distinctly deviating from those of the bulk liquid and these motions play an important role in regulating protein dynamics and functionality. Other techniques, such as Raman optical activity, INS, and computer simulations have been used to probe and describe the motions occurring in the protein and at the interfacial region with the solvent.

A simulation of the globular protein cytochrome c (Simonson and Perahia, 1996) has shown that the protein bulk and interfacial regions have different dielectric properties. Collective motion of the charged protein side chains, which undergo large-amplitude diffusive motion, makes the largest contribution to the permittivity at frequencies below 25 cm^{-1}, and motions of the backbone at frequencies as high as 60 cm^{-1}. It is tempting to assign the lowest frequency Brownian oscillators in the fits to the OHD-RIKES spectra to diffusive collective modes involving the side chains, and the higher frequency oscillators to motions of the protein backbone. The effective resolution in our spectra is $\sim$9 cm^{-1} and therefore very low frequency diffusive motions will not appear in the spectra.

The OHD-RIKES spectra can be compared with depolarized Raman and INS spectra by dividing them by the Bose thermal-occupation factor (Orecchini et al., 2001) (See Eq. 2). Fig. 6 shows the depolarized Raman spectra obtained by conversion of the OHD-RIKES spectrum of lysozyme and SF lysozyme. In previous studies of the low-frequency Raman spectrum of lysozyme (Genzel et al., 1976), two peaks at 25 and 75 cm^{-1} were observed in the crystalline state whereas only a bump at 75 cm^{-1} was observed in aqueous solution. The disappearance of the 25-cm^{-1} band in solution suggested that this mode was either a lattice vibration (a phonon mode) rather than a mode of the protein itself or heavily overdamped in solution. The depolarized Raman spectrum obtained by conversion of the OHD-RIKES spectrum of lysozyme in water solution shown in Fig. 6 exactly reproduces the spontaneous Raman scattering result (Genzel et al., 1976). However, the SF OHD-RIKES spectrum of lysozyme converted to a depolarized spontaneous Raman scattering spectrum, does show a peak at both 25 and 75 cm^{-1}. This shows that the 25-cm^{-1} mode neither is a lattice mode nor is it overdamped.

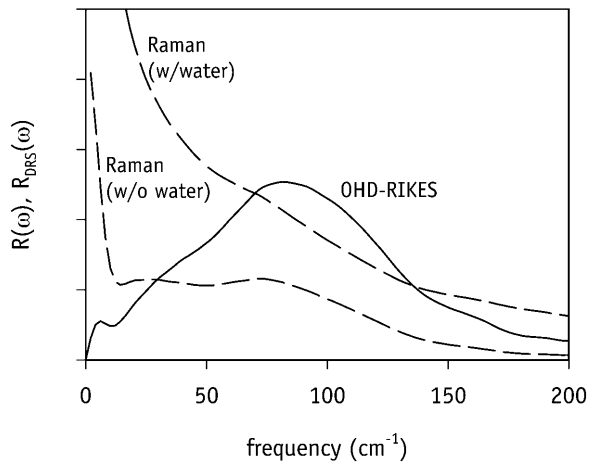

FIGURE 6 The solvent-free OHD-RIKES spectrum of lysozyme in aqueous solution and OHD-RIKES spectra converted to depolarized Raman spectra. The dashed lines show the depolarized Raman spectra obtained by converting OHD-RIKES spectra of lysozyme in aqueous solution with and without the solvent spectrum subtracted. The raw Raman spectrum is fully consistent with earlier Raman spectroscopic studies on lysozyme (Genzel et al., 1976) and shows the earlier observed band at 75 cm^{-1}.

A number of INS studies have been performed on proteins such as myoglobin (Diehl et al., 1997), lysozyme (Diehl et al., 1997), and β-lactoglobulin (Orecchini et al., 2001) in which the low-frequency vibrational density of states has been measured. All of these spectra exhibit a broad band centered at around 25 cm^{-1} that is usually referred to as the ''boson peak.'' The INS spectrum is proportional to the density of states of vibrational modes involving hydrogen atoms (Middendorf, 1984; Orecchini et al., 2001). A depolarized spontaneous Raman-scattering spectrum is also proportional to the vibrational density of states (involving any type of atom) but multiplied by the square of the derivative of the polarizability tensor (Cho et al., 1993). Therefore, the spectral dependence ought to be the same in both types of spectra. In INS, it is straightforward to obtain a solvent-free spectrum by using D_2O as the solvent (the scattering cross section for D is 10 times lower than for H). Hence, a SF OHD-RIKES spectrum converted to a depolarized Raman spectrum is directly comparable to the equivalent INS spectrum. It is clear that the peak in the SF Raman spectrum at $\sim$25 cm^{-1} corresponds directly with the boson peak in INS. In fact, the argument is stronger. The low-frequency INS spectrum of β-lactoglobulin (Orecchini et al., 2001) has been fitted to a Lorentzian $[(\omega-\omega_0)^2+\sigma^2]^{-1}$ with a center frequency of $\omega_0 = 3$ meV (24 cm^{-1}) and a width of $\sigma = 3.8$ meV (21 cm^{-1}). Fig. 7 compares this fit to the INS data converted to an OHD-RIKES representation by use of the Boltzmann factor in Eq. 2 with the two lowest frequency Brownian-oscillator components of the fit to the SF OHD-RIKES spectrum of β-lactoglobulin shown in Fig. 5. Considering the uncertainties involved in fitting the OHD-RIKES spectra (see above), the correspondence in Fig. 7 is surprisingly good.

All published INS spectra of globular proteins (Diehl et al., 1997; Orecchini et al., 2001) show the Boson peak at $\sim$25 cm^{-1}. It is logical to assume that the Boson peak in INS corresponds with the lowest frequency Brownian oscillator out of the triplet used to fit the OHD-RIKES spectra shown in Fig. 5. The OHD-RIKES spectra converted to spontaneous Raman spectra show an additional peak (corresponding

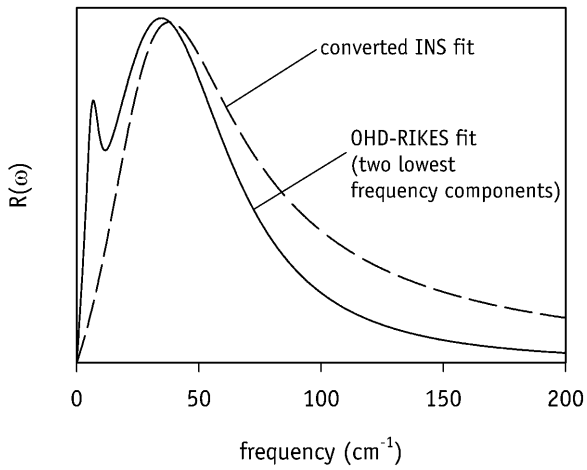

FIGURE 7 (*Dashed line*) A fit to the INS spectrum of β-lactoglobulin (Orecchini et al., 2001) converted to an OHD-RIKES representation by use of the Boltzmann factor Eq. 2. (*Solid line*) The two lowest frequency Brownian-oscillator components of the fit to the SF OHD-RIKES spectrum of β-lactoglobulin shown in Fig. 5.

to two additional Brownian oscillators) at around 80 cm^{-1}. These two additional modes are not observed in INS spectra. The signal strength in INS is proportional to the density of states of vibrational modes that involve motion of the hydrogen atoms, whereas Raman scattering scales with the density of states times the square of the polarizability derivative. Therefore, it is concluded that the modes around 80 cm^{-1} do not involve significant motion of hydrogen atoms or that they involve hydrogen motion with a large polarizability derivative for a small density of states. This largely excludes involvement of large amplitude delocalized motion of the secondary structure and strongly suggests that the dynamics responsible for the broad peak around 80 cm^{-1} involves mostly motion of the protein backbone. This would be in agreement with previous computer simulations of the permittivity of cytochrome c (Simonson and Perahia, 1996).

INS experiments can discriminate between the dynamics of polar residues on the surface of a protein and the nonpolar residues in its core by using deuterium-exchange. Additionally, the technique can separate diffusive overdamped motions from underdamped vibrations by varying the degree of hydration and temperature in the sample. An INS study of lysozyme and myoglobin (Diehl et al., 1997) shows that at room temperature the amplitude of the diffusive region strongly depends on the level of hydration implying the involvement of overdamped motion of the solvent-exposed side chains. This is consistent with the data presented here that show a low frequency spectrum largely independent of the type of secondary structure of the protein. A recent study of β-lactoglobulin (Orecchini et al., 2001) suggests that the solvent-exposed side chains of the protein undergo overdamped diffusive libration resulting in a low frequency component around 10 cm^{-1} whereas the nonpolar groups follow an underdamped libration at higher frequency around 25 cm^{-1}.

The low-frequency spectrum could also have an origin in strong hydrogen-bond interaction between the protein and water. As discussed above, Raman optical-activity measurements have suggested (Barron et al., 1997) that individual residues in disordered loop regions of molten globule-like states cluster in different secondary structure regions, and that they flicker between these regions at rates $\sim 10^{12}$ s^{-1} ($\sim$30 cm^{-1}). It has been proposed that the same dynamical behavior could occur in certain regions of native folded proteins. According to simulations (Zhou et al., 1998), such fast fluctuations could occur close to the active site of an enzyme. From the point of view of the protein functionality, the flickering of residues close to the active site could drive a rapid switching of the protein gate that is required for the proper functioning of conformational gating as a mechanism for enzyme specificity.

CONCLUSION

A typical chemical reaction takes place on a timescale of about a picosecond. Therefore, motion of a protein occurring on a similar timescale (corresponding to the frequency range 0–200 cm^{-1}) will affect protein activity. To investigate the dynamic motions on that timescale and its relation to structure, three model systems of increasing complexity have been studied with OHD-RIKES spectroscopy. The two peptides di-L-alanine and poly-L-alanine have been chosen to study the influence of primary and secondary structure. Four globular proteins have been chosen to study the possible influence of secondary and tertiary structure. The spectra of di-L-alanine and poly-L-alanine have shown a common feature above 100 cm^{-1}. Below 100 cm^{-1} extra amplitude is present in the PLA spectrum suggesting an origin in the secondary structure. Possible explanations for this extra amplitude include i), vibrational motion in the helix becoming Raman active through the polarizability anisotropy induced by the electric field associated with the helical structure and ii), fast ($\sim$1 ps) flickering between secondary-structure regions.

A set of two mostly α-helical proteins, lysozyme and α-lactalbumin, has been compared to a set of two mostly β-sheet proteins, β-lactoglobulin and pepsin. The four globular proteins present very similar spectra. This shows that there is no clear signature of the type of secondary structure at low frequency ($<$200 cm^{-1}). Three main features could be isolated. At very low frequency ($<$10 cm^{-1}), a purely diffusive component is observed in two of the samples studied. Between 20 and 40 cm^{-1} a shoulder, recognized as the boson peak seen in INS spectra, accounts for heavily damped librational motion of solvent-exposed side chains and perhaps the flickering between different regions of the secondary structure around the active site. Finally, a peak centered around 80 cm^{-1} that does not appear in INS spectra

and may be associated with delocalized backbone torsions not involving motion of the hydrogen atoms to a great degree.

In conclusion, OHD-RIKES spectroscopy has proven to be a reliable technique for the study low frequency vibrational dynamics of biological system. This type of Raman spectroscopy is especially powerful when spectra can be compared with those obtained from INS and other spectroscopies. Further improvements in the signal-to-noise ratio of OHD-RIKES experiments and variants such as polarization-selective femtosecond Raman techniques (Eaves et al., 2003) will allow a further disentanglement of the low frequency spectra of proteins.

We thank L. D. Barron and I. H. McColl for useful discussions.

We thank the Engineering and Physical Sciences Research Council (EPSRC) for financial support. Acknowledgment is also made to the donors of The Petroleum Research Fund, administered by the ACS for support of this research.

REFERENCES

Bamford, C. H., A. Elliott, and W. E. Hanby. 1956. Synthetic Polypeptides: Preparation, Structure, and Properties. Academic Press, New York.

Barron, L. D., L. Hecht, and G. Wilson. 1997. The lubricant of life: a proposal that solvent water promotes extremely fast conformational fluctuations in mobile heteropolypeptide structure. *Biochemistry*. 36: 13143–13147.

Beard, M. C., G. M. Turner, and C. A. Schmuttenmaer. 2002. Terahertz spectroscopy. *J. Phys. Chem. B*. 106:7146–7159.

Berman, H. M., J. Westbrook, Z. Feng, G. Gilliland, T. N. Bhat, H. Weissig, I. N. Shindyalov, and P. E. Bourne. 2000. The Protein Data Bank. *Nucleic Acids Res*. 28:235–242.

Bon, C., A. J. Dianoux, M. Ferrand, and M. S. Lehmann. 2002. A model for water motion in crystals of lysozyme based on an incoherent quasielastic neutron-scattering study. *Biophys. J*. 83:1578–1588.

Cho, M., M. Du, N. F. Scherer, G. R. Fleming, and S. Mukamel. 1993. Off-resonant transient birefringence in liquids. *J. Chem. Phys*. 99:2410–2428.

Crupi, V., D. Majolino, P. Migliardo, and V. Venuti. 2002. Low-frequency dynamics in confined water: a comparative analysis by Raman and inelastic neutron scattering. *Philos. Mag. B-Phys. Condens. Matter Stat. Mech. Electron. Opt. Magn. Prop*. 82:425–430.

Daune, M. 1999. Molecular Biophysics: Oxford University Press.

Diehl, M., W. Doster, W. Petry, and H. Schober. 1997. Water-coupled low-frequency modes of myoglobin and lysozyme observed by inelastic neutron scattering. *Biophys. J*. 73:2726–2732.

Eaves, J. D., C. J. Fecko, A. L. Stevens, P. Peng, and A. Tokmakoff. 2003. Polarization-selective femtosecond raman spectrocopy of low-frequency motions in hydrated protein films. *Chem. Phys. Lett*. 376:20–25

Ferretti, J. A., and L. Paolillo. 1969. Nuclear magnetic resonance investigation of the helix to random coil transformation in poly-alpha-amino acids. *Biopolymers*. 7:155–171.

Fischer, S., J. C. Smith, and C. S. Verma. 2001. Dissecting the vibrational entropy change on protein/ligand binding: Burial of a water molecule in bovine pancreatic trypsin inhibitor. *J. Phys. Chem. B*. 105:8050–8055.

Genzel, L., F. Keilmann, T. P. Martin, G. Winterling, Y. Yacoby, H. Frohlich, and M. Makinen. 1976. Low-frequency Raman spectra of lysozyme. *Biopolymers*. 15:219–225.

Giraud, G., C. M. Gordon, I. R. Dunkin, and K. Wynne. 2003. The effect of anion and cation substitution on the ultrafast solvent dynamics of ionic liquids: a time-resolved optical Kerr-effect spectroscopic study. *J. Chem. Phys*. 119:464–477.

Giraud, G., and K. Wynne. 2002. Time-resolved optical Kerr-effect spectroscopy of low-frequency dynamics in Di-L-alanine, poly-L-alanine, and lysozyme in solution. *J. Am. Chem. Soc*. 124:12110–12111.

Gold, D. G., and W. G. Miller. 1999. Polymer Data Handbook: Oxford University Press.

Groot, M. L., M. H. Vos, I. Schlichting, F. van Mourik, M. Joffre, J. C. Lambry, and J. L. Martin. 2002. Coherent infrared emission from myoglobin crystals: An electric field measurement. *Proc. Natl. Acad. Sci. USA*. 99:1323–1328.

Hammes-Schiffer, S. 2002. Impact of enzyme motion on activity. *Biochemistry*. 41:13335–13343.

Hol, W. G. J., P. T. van Duijnen, and H. J. C. Berendsen. 1978. The alpha-helix dipole and the properties of proteins. *Nature*. 273:443–446.

Jimenez, R., D. A. Case, and F. E. Romesberg. 2002. Flexibility of an antibody binding site measured with photon echo spectroscopy. *J. Phys. Chem. B*. 106:1090–1103.

Jung, Y. M., B. Czarnik-Matusewicz, and Y. Ozaki. 2000. Two-dimensional infrared, two-dimensional Raman, and two- dimensional infrared and Raman heterospectral correlation studies of secondary structure of beta-lactoglobulin in buffer solutions. *J. Phys. Chem. B*. 104:7812–7817.

Kubo, R. 1969. A stochastic theory of lineshape. *Adv. Chem. Phys*. 15:101–127.

Kuwata, K., M. Hoshino, V. Forge, S. Era, C. A. Batt, and Y. Goto. 1999. Solution structure and dynamics of bovine beta-lactoglobulin A. *Protein Sci*. 8:2541–2545.

Lee, S. H., and S. Krimm. 1998a. Polarized Raman spectra of oriented films of alpha-helical poly(L-alanine) and its N-deuterated analogue. *J. Raman Spectrosc*. 29:73–80.

Lee, S.-H., and S. Krimm. 1998b. Ab initio-based vibrational analysis of alpha-poly(L-alanine). *Biopolymers*. 46:283–317.

Levitt, M., C. Sander, and P. S. Stern. 1985. Protein normal-mode dynamics - trypsin-inhibitor, crambin, ribonuclease and lysozyme. *J. Mol. Biol*. 181:423–447.

McKenzie, H. A., and F. H. White. 1991. Lysozyme and alpha-lactalbumin - structure, function, and interrelationships. *Adv. Protein Chem*. 41:173–315.

McMorrow, D. 1991. Separation of nuclear and electronic contributions to femtosecond four-wave-mixing data. *Opt. Commun*. 86:236–244.

McMorrow, D., and W. T. Lotshaw. 1990. The frequency-response of condensed-phase media to femtosecond optical pulses - spectral-filter effects. *Chem. Phys. Lett*. 174:85–94.

McMorrow, D., W. T. Lotshaw, and G. A. Kenney-Wallace. 1988. Femtosecond optical Kerr studies on the origin of the nonlinear responses in simple liquids. *IEEE J. Quantum Electron*. 24:443–454.

Middendorf, H. D. 1984. Biophysical applications of quasi-elastic and inelastic neutron-scattering. *Annu. Rev. Biophys. Bioeng*. 13:425–451.

Nakabayashi, T., K. Kosugi, and N. Nishi. 1999. Liquid structure of acetic acid studied by Raman spectroscopy and ab initio molecular orbital calculations. *J. Phys. Chem. A*. 103:8595–8603.

Orecchini, A., A. Paciaroni, A. R. Bizzarri, and S. Cannistraro. 2001. Low-frequency vibrational anomalies in beta-lactoglobulin: contribution of different hydrogen classes revealed by inelastic neutron scattering. *J. Phys. Chem. B*. 105:12150–12156.

Paciaroni, A., A. R. Bizzarri, and S. Cannistraro. 1999. Neutron scattering evidence of a boson peak in protein hydration water. *Phys. Rev. E*. 60:R2476–R2479.

Pethig, R. 1992. Protein-water interactions determined by dielectric methods. *Annu. Rev. Phys. Chem*. 43:177–205.

Press, W. H., S. A. Teukolsky, W. T. Vetterling, and B. P. Flannery. 1992. Numerical Recipes in C. Cambridge University Press.

Rosca, F., A. T. N. Kumar, D. Ionascu, X. Ye, A. A. Demidov, T. Sjodin, D. Wharton, D. Barrick, S. G. Sligar, T. Yonetani, and P. M. Champion.

2002. Investigations of anharmonic low-frequency oscillations in heme proteins. *J. Phys. Chem. A.* 106:3540–3552.

Seber, G. A., and C. J. Wild. 1989. Nonlinear Regression. Wiley, New York.

Sielecki, A. R., A. A. Fedorov, A. Boodhoo, N. S. Andreeva, and M. N. G. James. 1990. Molecular and crystal-structures of monoclinic porcine pepsin refined at 1.8-Å resolution. *J. Mol. Biol.* 214:143–170.

Simonson, T., and D. Perahia. 1996. Polar fluctuations in proteins: molecular-dynamic studies of cytochrome c in aqueous solution. *Faraday Discuss.* 103:71–90.

Smith, N. A., and S. R. Meech. 2002. Optically-heterodyne-detected optical Kerr effect (OHD-OKE): applications in condensed phase dynamics. *Int. Rev. Phys. Chem.* 21:75–100.

Vaney, M. C., S. Maignan, M. Rieskautt, and A. Ducruix. 1996. High-resolution structure (1.33 angstrom) of a HEW lysozyme tetragonal crystal grown in the APCF apparatus. Data and structural comparison with a crystal grown under microgravity from SpaceHab-01 mission. *Acta Crystallogr. D-Biol. Crystallogr.* 52:505–517.

Wood, K. A., and H. L. Strauss. 1990. Broadening a nd shifts of vibrational bands due to the effect of thermal chemical-reactions. *J. Phys. Chem.* 94:5677–5684.

Woutersen, S., and P. Hamm. 2001. Time-resolved two-dimensional vibrational spectroscopy of a short alpha-helix in water. *J. Chem. Phys.* 115:7737–7743.

Wynne, K., J. J. Carey, J. Zawadzka, and D. A. Jaroszynski. 2000. Tunneling of single-cycle terahertz pulses through waveguides. *Opt. Commun.* 176:429–435.

Xie, A., L. van der Meer, and R. H. Austin. 2002. Excited-state lifetimes of far-infrared collective modes in proteins. *J. Biol. Phys.* 28:147–154.

Xie, A. H., L. Kelemen, J. Hendriks, B. J. White, K. J. Hellingwerf, and W. D. Hoff. 2001. Formation of a new buried charge drives a large-amplitude protein quake in photoreceptor activation. *Biochemistry.* 40:1510–1517.

Zanni, M. T., and R. M. Hochstrasser. 2001. Two-dimensional infrared spectroscopy: a promising new method for the time resolution of structures. *Curr. Opin. Struct. Biol.* 11:516–522.

Zanni, M. T., J. Stenger, M. C. Asplund, and R. M. Hochstrasser. 2001. Solvent dependent conformational dynamics of dipeptides studied with two-dimensional infrared spectroscopy. *Biophys. J.* 80:38.

Zhou, H. X., S. T. Wlodek, and J. A. McCammon. 1998. Conformation gating as a mechanism for enzyme specificity. *Proc. Natl. Acad. Sci. USA.* 95:9280–9283.